Microelectronics Reliability 51 (2011) 43–52

Contents lists available at ScienceDirect

Microelectronics Reliability

journal homepage: www.elsevier.com/locate/microrel

Effect of gas type and flow rate on Cu free air ball formation in thermosonic wire bonding

A. Pequegnat [a,*], H.J. Kim [a], M. Mayer [a], Y. Zhou [a], J. Persic [b], J.T. Moon [c]

[a] Centre for Advanced Materials Joining, University of Waterloo, ON, Canada N2L 3G1
[b] Microbonds Inc., Markham, Canada
[c] MK Electron Co. Ltd., Yongin, Republic of Korea

ARTICLE INFO

Article history:
Received 21 January 2010
Received in revised form 25 February 2010
Accepted 25 February 2010
Available online 20 March 2010

ABSTRACT

The development of novel Cu wires for thermosonic wire bonding is time consuming and the effects of shielding gas on the electrical flame off (EFO) process is not fully understood. An online method is used in this study for characterizing Cu free air balls (FABs) formed with different shielding gas types and flow rates. The ball heights before (H_{FAB}) and after deformation (H_{def}) are responses of the online method and measured as functions of gas flow rate. Sudden changes in the slopes of these functions, a non-parallelity of the two functions, and a large standard deviation of the H_{FAB} measurements all identify FAB defects. Using scanning electron microscope (SEM) images in parallel with the online measurements golf-club shaped and pointed shaped FABs are found and the conditions at which they occur are identified. In general FAB defects are thought to be caused by changes in surface tension of the molten metal during EFO due to inhomogeneous cooling or oxidation. It is found that the convective cooling effect of the shielding gas increases with flow rate up to 0.65 l/min where the bulk temperature of a thermocouple at the EFO site decreases by 19 °C. Flow rates above 0.7 l/min yield an undesirable EFO process due to an increase in oxidation which can be explained by a change in flow from laminar to turbulent. The addition of H_2 to the shielding gas reduces the oxidation of the FAB as well as providing additional thermal energy during EFO. Different Cu wire materials yield different results where some perform better than others.

1. Introduction

The general trends in the microelectronics industry include miniaturization, higher performance, and lower costs [1]. These trends are driving the research and development of low-cost packaging solutions for fine-pitch, high performance devices. Gold wire bonding is the most popular method for making electrical interconnections to integrated circuits used today [1,2]. The wire bonding industry is investigating new wire types and materials in order to meet industry demands.

Copper wire has become a very promising alternative due to its potentials for economical and performance advantages. Relative to Au wire, Cu wire has superior electrical and thermal conductivities as well as higher tensile strength and elongation [1–3]. The superior material properties of Cu wire make it better suited for fine-pitch and high performance applications. Copper wire has two main drawbacks that have retarded its replacement of Au wire. Copper wire is harder than Au wire and oxidizes in air. The high hardness of Cu wire increases the occurrence of chip damage during bonding [1,3,4]. Research focusing on methods of softening the Cu wire and its free air ball (FAB) during bonding were reported in [5–7]. This paper focuses on oxidation and the complications associated with adding a shielding gas to the electrical flame off (EFO) process. Excessive oxidation can lead to process reliability issues and further increases the hardness of the Cu FAB [2,8–10]. The oxidation of Cu wire during bonding is reduced by supplying a shielding gas to the EFO site during FAB formation. The shielding gasses used are usually a mixture of H_2 and an inert gas such as Ar or N_2 (forming gas) [11]. A mixture of 5% H_2 and 95% N_2 is the most common forming gas mixture used today. The hydrogen in the gas mixture reduces the oxide on the wire surface during the EFO process [9]. Mixtures containing larger than 5% H_2 are considered flammable and are avoided for safety and handling purposes [11].

The melting and solidification of the FAB during the EFO process has been studied extensively for Au wire. Complex models have been developed to help understand the formation of the Au FAB during EFO [12]. The formation of a Cu FAB is even more complex due to the effects of oxidation and the use of a shielding gas. Factors such as extensive oxidation and convective cooling affect the formation of the FAB and can cause FAB defects [2,9,13]. Forming gas reduces the oxidation of the Cu FAB but is an additional expense and a safety concern for the wire bonding industry. A novel Cu alloy or wire type that can eliminate the need for H_2 in the shielding gas or even eliminate the shielding gas all together would be a huge breakthrough for Cu wire bonding. However, developing

* Corresponding author.
E-mail address: apequegn@uwaterloo.ca (A. Pequegnat).

0026-2714/$ - see front matter © 2010 Elsevier Ltd. All rights reserved.
doi:10.1016/j.microrel.2010.02.023

new wires is very time consuming and there is not yet a solid understanding of how the shielding gas effects the formation of the Cu FAB.

Online methods have been developed to characterize wire deformation/hardness and the resulting in situ underpad stresses during bonding [4,14]. They are especially useful for characterizing new prototype wires and optimizing process parameters [4,7,14–17]. A prototype wire that does not meet certain standards can be discarded early preventing wasted time performing tedious manual characterization techniques. In this study, an online method is used that can characterize the shape and deformability of 380 FABs in 1 h. This online FAB characterization method is used in parallel with scanning electron microscope (SEM) images to develop a method of determining optimal shielding gas flow rates using 5% H_2 + 95% N_2 forming gas and a 100% N_2 gas. The common types of FAB defects and the conditions at which they occur are identified. Parts of this study are published in the proceedings of the International Microelectronics and Packaging Society (IMAPS), 42nd International Symposium on Microelectronics [16].

2. Experimental procedure

Various 25 μm diameter wires are used along with the SBNE-35BD-AZM-1/16-XL capillary manufactured by Small Precision Tools Ltd., Lyss, Switzerland. Two different Cu wires were chosen (Cu1 and Cu2) as well as a Au wire that is used as the base case where oxidation is not a factor during EFO. All of the bonding is performed on Ag plated Cu leadframes using an automated ESEC 3100 thermosonic wire bonder, manufactured by Besi ESEC, Cham, Switzerland. The EFO performance of each of the wires is investigated using the 5% H_2 + 95% N_2 forming gas as well as an inert N_2 gas.

The EFO parameters are optimized to give a FAB diameter of approximately 50 μm [7]. Sets of EFO parameters are found for each wire in the forming gas and N_2 gas atmospheres and are presented in Table 1. A larger EFO current is required for forming the Cu FABs due to the superior thermal conductivity of Cu compared to Au.

For the online FAB characterization method, an encoder measures the bondhead position with sub-micron precision along the *z*-axis [14,16]. The *z*-position of the capillary tip is derived from the encoder measurements and recorded during bonding. Rows of ball-stitch bonds are made where the *z*-position is used to derive a reference height (H_{ref}) of the bonding surface, the Z_1 height of the undeformed FAB, and the Z_2 height of the deformed FAB as shown in Fig. 1. The Z_1 height is taken when the FAB is touched down with 20 mN force. The 20 mN force is too low to cause significant deformation of the FAB [17]. The Z_2 height is taken after the FAB has been deformed with a force of 600 mN. This is a suitable force value for the type of wire and materials used. Once the Z_2 height has been measured, the deformed ball is bonded by applying the bonding force and ultrasound (US) in order to complete the process. The FAB height (H_{FAB}) can now be calculated using

$$H_{FAB} = Z_1 - H_{ref} \quad (1)$$

Table 1
EFO Parameters for 50 μm diameter FAB using forming gas and N_2 gas with a shielding gas flow rate of 0.5 l/min and a tail length of 500 μm.

	EFO parameters: forming gas			EFO parameters: N_2 gas		
	Cu1	Cu2	Au	Cu1	Cu2	Au
Electrode to wire distance (μm)	300	300	500	300	300	500
EFO current (mA)	80	80	52	80	80	52
EFO time (ms)	0.43	0.43	0.5	0.46	0.46	0.51

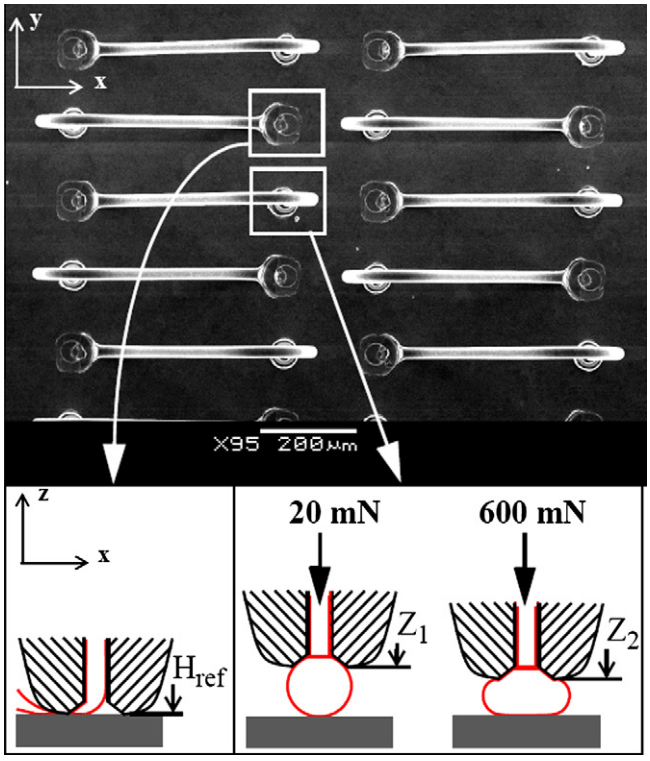

Fig. 1. Rows of ball-stitch bonds for height measurement and schematic illustration of reference height Z_1, and Z_2 measurements.

and the deformed ball height (H_{def}) can be calculated using

$$H_{def} = Z_2 - H_{ref} \quad (2)$$

The H_{FAB} and H_{def} measurements are taken for each of the three wire types using both forming gas and N_2 gas. The wire bonder is not capable of reading flow rates below 0.2 l/min and flow rates above 1.0 l/min promotes severely defective FABs and non-stick on pad (NSOP) failures where ball bonds cannot be made. Therefore, a total of 180 ball-stitch bonds are made at each of the flow rates from 0.2 l/min to 1.0 l/min at 0.05 l/min increments.

SEM images are used to characterize the FABs size, shape, and surface condition at various flow rates. SEM images also help identify the possible mechanism for a defective FAB. Free air ball defects such as variation in diameter or shape are identified using the online method in parallel with SEM images. Observed shapes are spherical, pointed, or golf-clubbed, as illustrated in Fig. 2a, b, and c, respectively. In the spherical case, the ball is spherical and the wire axis projects through the ball center. In the pointed case, the ball shape has a point usually at the far end from the wire. While the ball might be almost spherical in the golf-clubbed case, its center point is substantially of the extended wire axis.

Oxidation of the surface of the molten Cu FAB or excessive forced convective cooling due to high shielding gas flow rates can produce these FAB defects [13]. The forced convective cooling effect is measured using a thermocouple while increasing the flow rate of the shielding gas as shown in Fig. 3. A k-type (chromel–alumel) thermocouple manufactured by OMEGA, Laval, Quebec, Canada, is used.

3. Results

3.1. FABs produced in forming gas

3.1.1. Copper wire 1 (Cu1)

The FABs are characterized using the online FAB characterization method in parallel with SEM images. The results for the online

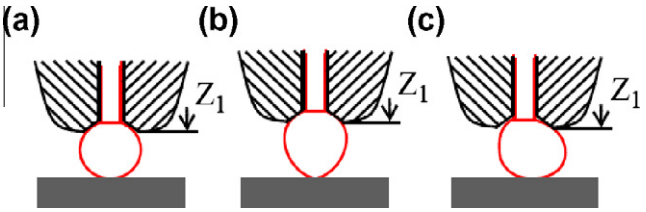

Fig. 2. Common, FAB shapes: (a) spherical FAB, (b) pointed FAB defect, and (c) golf-clubbed FAB defect.

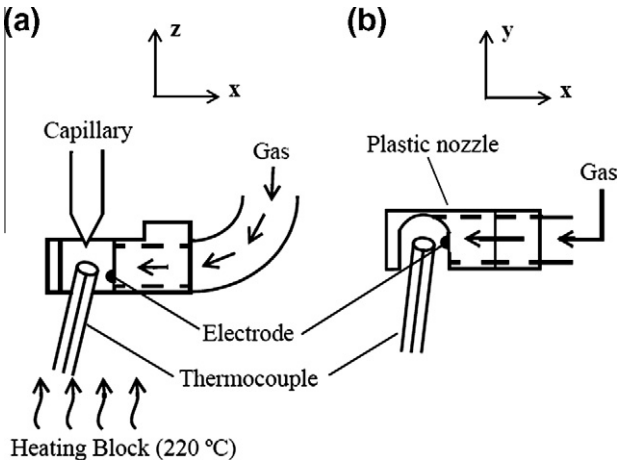

Fig. 3. Setup for measuring forced convective cooling effect of shielding gas with increasing flow rate: (a) front view of electrode and (b) top view of electrode.

FAB characterization are shown in Fig. 4. From the online measurements no monotonic trend in H_{FAB} is observed with increasing the flow rate. For flow rates above 0.7 l/min, the H_{FAB} does not change and the standard deviation increases drastically.

Using SEM images the actual shape and quality of the FAB is determined at each of the different flow rates. From the SEM images in Fig. 5a and c, it can be seen that the FAB is of good quality at flow rates of 0.2 l/min and 0.5 l/min. The standard deviation of the H_{FAB} measurements are the lowest at 0.2 l/min and 0.5 l/min with values of 0.44 μm and 0.51 μm, respectively. Insignificant surface oxidation is observed and the grain boundaries are clearly

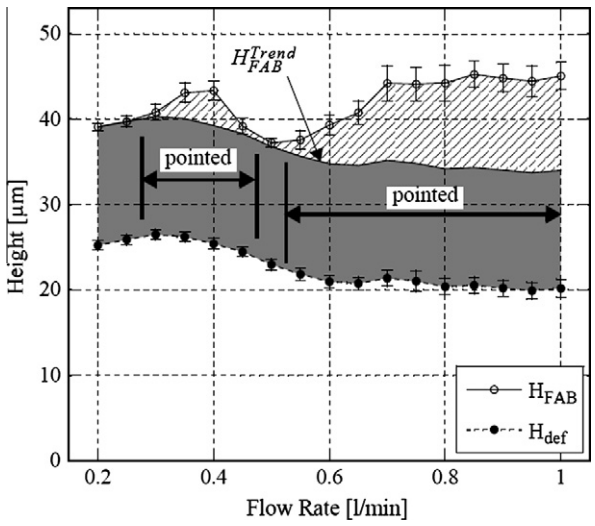

Fig. 4. Cu1 wire height measurements from online FAB characterization in forming gas. The mis-shaped FAB area is identified by the hatched region.

visible. The FABs are pointed at flow rates of 0.4 l/min and 0.75 l/min as shown in Fig. 5b and d, respectively. The standard deviation of the H_{FAB} measurements at flow rates of 0.4 l/min and 0.75 l/min increases to 1.08 μm and 1.95 μm, respectively. Oxidation is identified visually on the pointed FABs shown in Fig. 5b and d, where a scale-like oxide is observed on the FAB surface.

From the SEM images the changes in H_{FAB} measured using the online method are due to changes in the FAB shape, where as the H_{def} measurements are more dependent on the volume of the FAB. Spherical Au FABs with different H_{FAB} measurements are deformed and plotted against the H_{def} measurements as shown in Fig. 6. A linear correlation is found between the H_{FAB} and H_{def} measurements and with a deformation force of 600 mN the slope approaches unity. Therefore, in a process where a spherical FAB is produced at all flow rates, the H_{FAB} measurements only vary due to changes of FAB diameter and follow the same trend as the H_{def} measurements. Such H_{FAB} measurements are named H_{FAB}^{Trend} and are calculated by

$$H_{FAB}^{Trend} = H_{def} + \Delta H_{min} \quad (3)$$

where, ΔH_{min} is the minimum difference between H_{FAB} and H_{def} from all flow rates [16]. When H_{FAB} is approximately equal to H_{FAB}^{Trend} as illustrated in Fig. 5 for the Cu1 wire at flow rates of 0.2 l/min, 0.25 l/min and 0.5 l/min, the FAB is spherical and of good surface quality. All other flow rates where pointed FABs are produced are identified by the hatched area above H_{FAB}^{Trend} termed the mis-shaped FAB area [16].

3.1.2. Copper wire 2 (Cu2)

The results for the online FAB characterization of Cu2 are shown in Fig. 7. For the Cu2 wire there is an obvious trend in the H_{FAB} with increasing flow rate. This trend with increasing flow rate is similar to the results found by Ho et al. [13]. The FAB height increases from 0.2 l/min to 0.3 l/min before decreasing until a flow rate of 0.7 l/min. However, at flow rates above 0.7 l/min the slope in the H_{FAB} trend changes and H_{FAB} remains approximately constant.

Images of the FABs produced at various flow rates are shown in Fig. 8. The FABs produced with flow rates below 0.65 l/min are of good quality which correlates well with the low standard deviation values calculated from the online measurements. However, as seen in Fig. 8c and d, golf-clubbed defects start to occur at flow rates above 0.65 l/min. Also, at higher flow rates more severe oxidation is observed on the FAB, as observed in Fig. 8d.

The measured H_{FAB} values follow the calculated H_{FAB}^{Trend} values closely for all flow rates and the mis-shaped FAB area is small, as shown in Fig. 7. As expected this indicates that spherical FABs are produced. However, golf-clubbed defects occur at flow rates above 0.65 l/min even though the H_{FAB} measurements follow the H_{FAB}^{Trend} values closely. However, the slope in the H_{FAB} and H_{def} curves decreases at 0.65 l/min, indicating a change in the EFO process and the production of FAB defects.

3.1.3. Gold wire

Since Au does not oxidize the effects of the forming gas and the flow rate can be more easily identified. The online FAB characterization results are shown in Fig. 9. Since it is possible to bond Au FABs with no forming gas because oxidation is not an issue, the online characterization method is performed at a flow rate of 0 l/min. The H_{FAB} and H_{def} increase from flow rates of 0–0.25 l/min and then decrease steadily until about 0.65 l/min. This trend is again similar to the results found for the Cu2 wire and by Ho et al. [13].

The H_{FAB} and H_{FAB}^{Trend} values are similar for flow rates up to 0.5 l/min as shown in Fig. 9. Spherical FABs are produced at flow rates up to 0.5 l/min as shown in Fig. 10a and b. Above 0.5 l/min the FAB becomes golf-clubbed and at 0.8 l/min spherical FABs can no

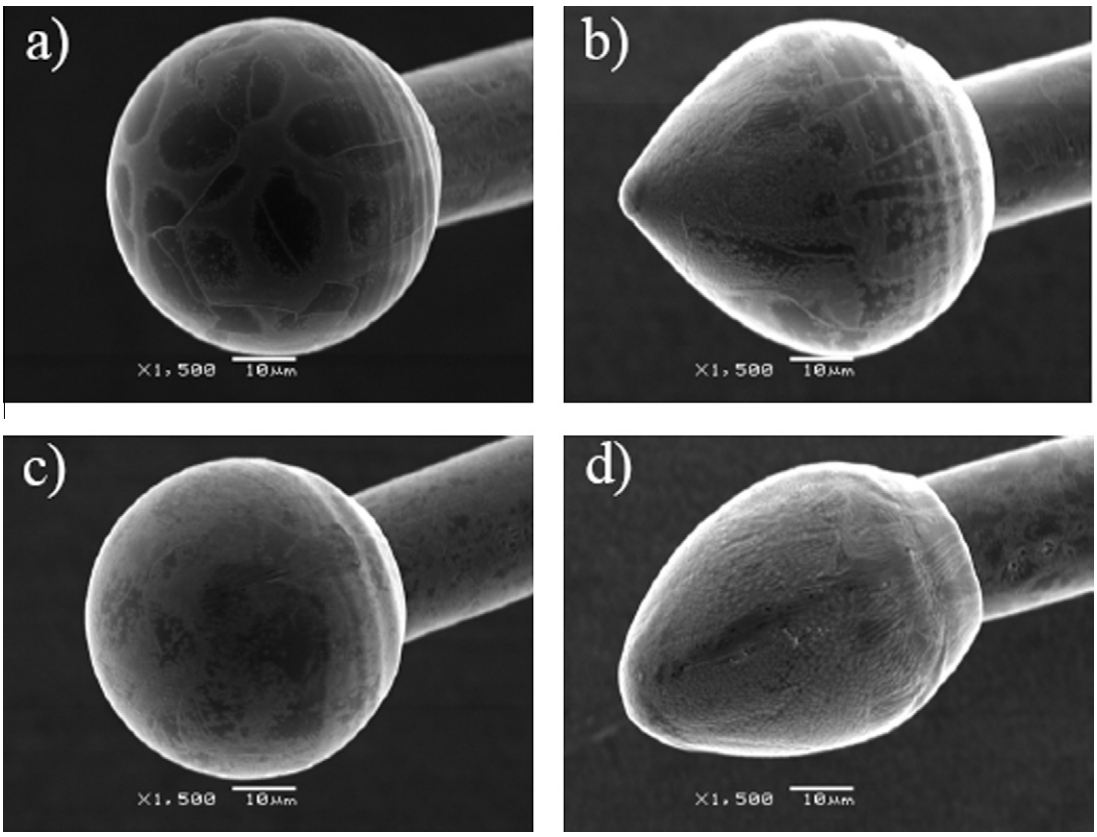

Fig. 5. SEM images of Cu1 FABs produced in forming gas at flow rates of: (a) 0.2 l/min, (b) 0.4 l/min, (c) 0.5 l/min, and (d) 0.75 l/min.

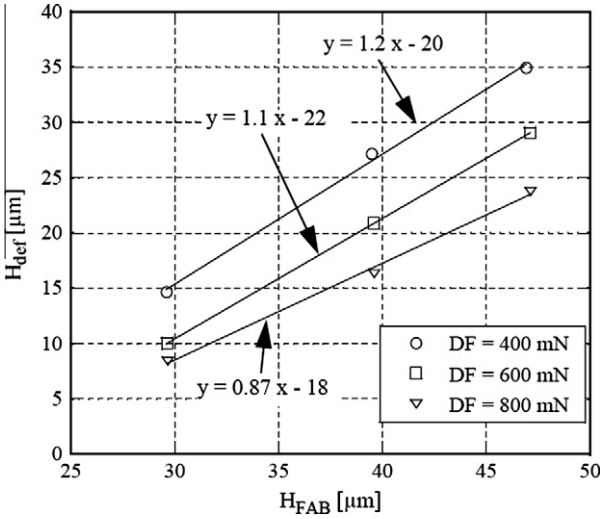

Fig. 6. Correlation between H_{FAB} and H_{def} measurements for various sized Au FABs deformed with deformation forces of 400, 600, and 800 mN.

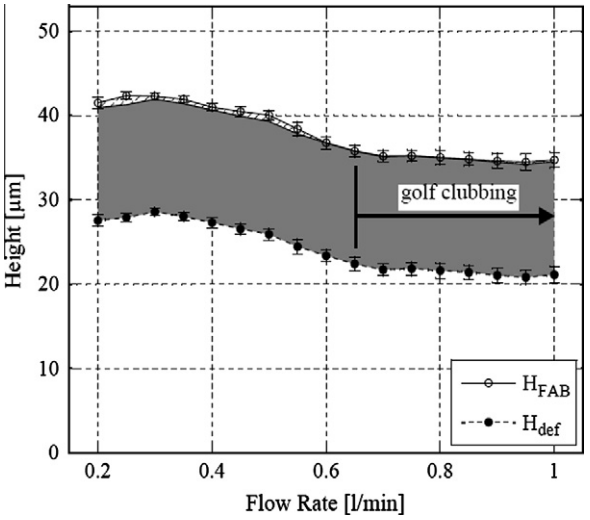

Fig. 7. Cu2 wire height measurements from online FAB characterization in forming gas. The mis-shaped FAB area is identified by the hatched region.

longer be formed as shown in Fig. 10c and d, respectively. At flow rates above 0.5 l/min the mis-shaped FAB area increases, and also, the slope in H_{FAB} and H_{def} changes at flow rates above 0.55 l/min where H_{FAB} remains constant.

3.2. FAB produced in nitrogen gas

3.2.1. Copper wire 1 (Cu1)

The quality of the FABs is expected to decrease when they are formed in N_2 gas. This is due to the fact that there is no H_2 present to reduce the Cu oxide during EFO. The online FAB characterization results in N_2 gas are shown in Fig. 11. The standard deviation of the H_{FAB} is approximately double that of the FABs produced in forming gas. An abrupt jump in H_{FAB} occurs at a 0.65 l/min flow rate and again, the H_{FAB} remains constant above a flow rate of 0.65 l/min.

SEM images of the Cu1 FABs produced in N_2 gas are shown in Fig. 12. Every FAB is defective and severe oxidation is observed on its surface. The FAB shapes changes from severely pointed at 0.2 l/min flow rate, to slightly ovalized at 0.55 l/min, and then again becomes pointed at a flow rate of 0.7 l/min.

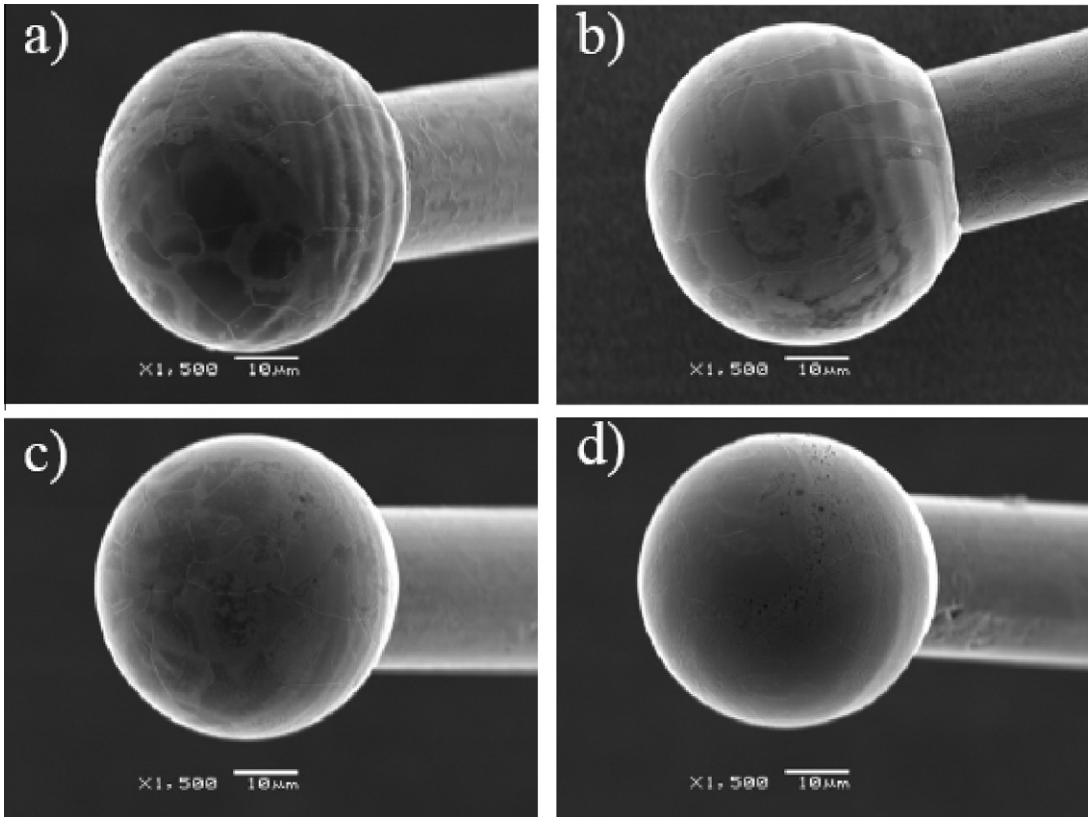

Fig. 8. SEM images of Cu2 FABs produced in forming gas at flow rates of: (a) 0.2 l/min, (b) 0.5 l/min, (c) 0.65 l/min, and (d) 0.8 l/min. Golf-clubbed shapes in (c and d) pointing towards observer.

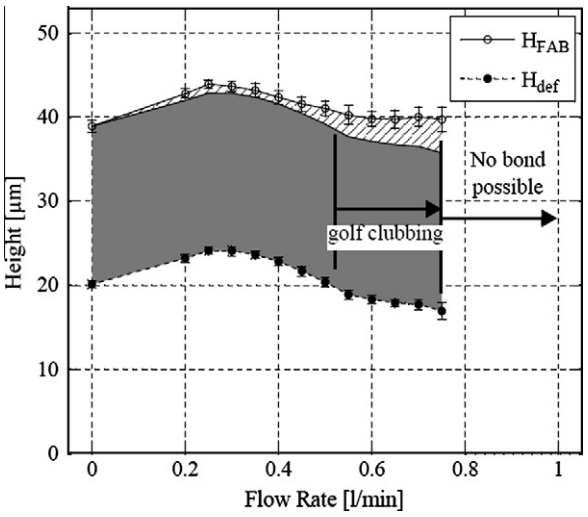

Fig. 9. Au wire height measurements from online FAB characterization in forming gas. The mis-shaped FAB area is identified by the hatched region.

The H_{FAB} and H_{def} trends have several changes in slope, and the mis-shaped FAB area is large. Therefore, it is expected that the FABs will be defective at all flow rates. With flow rates from 0.45 l/min to 0.55 l/min the FABs are golf-clubbed and the H_{FAB} and H_{FAB}^{Trend} values are similar but the slopes of the H_{FAB} and H_{def} trends change abruptly in this region identifying an unstable EFO process.

3.2.2. Copper wire 2 (Cu2)

The online FAB characterization results for the Cu2 FABs produced in N_2 gas are shown in Fig. 13. The online test could not be performed for flow rates below 0.4 l/min due to NSOP failures where ball bonds could not be made. The standard deviation of the H_{FAB} and H_{def} measurements is more than double that of the FABs produced with forming gas just as was observed with the Cu1 wire. The H_{FAB} and H_{def} measurements decrease up to 0.65 l/min where there is an abrupt increase in both.

The SEM images shown in Fig. 14 again reveal oxidation of the FABs produced in N_2 gas. The Cu2 wire tends to form golf-clubbed defects varying in severity at all N_2 gas flow rates. Golf clubbing and significant surface oxidation occurs at flow rates below 0.4 l/min where NSOP failures occur and also above 0.65 l/min where the online H_{FAB} and H_{def} measurements increase abruptly.

From the online results shown in Fig. 13 the mis-shaped FAB area is observed to be large. Only golf-clubbed FABs were observed with the Cu2 wire when formed in N_2 gas. The H_{FAB} and H_{FAB}^{Trend} values are equal at 0.4 l/min but spherical FABs were not produced. If the ΔH_{min} used to calculate the H_{FAB}^{Trend} value is from an unstable EFO process where FAB defects occur, H_{FAB}^{Trend} cannot be used to identify flow rates where spherical FABs are produced. Since FAB defects were produced at all flow rates in this case, no conclusion can be made from H_{FAB} being equal to H_{FAB}^{Trend}.

3.2.3. Gold wire

The two main purposes of studying Au FAB formation in N_2 gas is to understand how the gas flow effects the FAB formation and also to understand the effects of not having H_2 in the gas mixture. The online FAB characterization results for the Au wire are shown in Fig. 15. The H_{FAB} and H_{def} both decrease with N_2 gas. The H_{FAB} decreases up to a flow rate of 0.25 l/min before it increases slightly. The standard deviation increases drastically at 0.4 l/min and bonding could not be done at flow rates above 0.5 l/min due to a drastic decrease in FAB size.

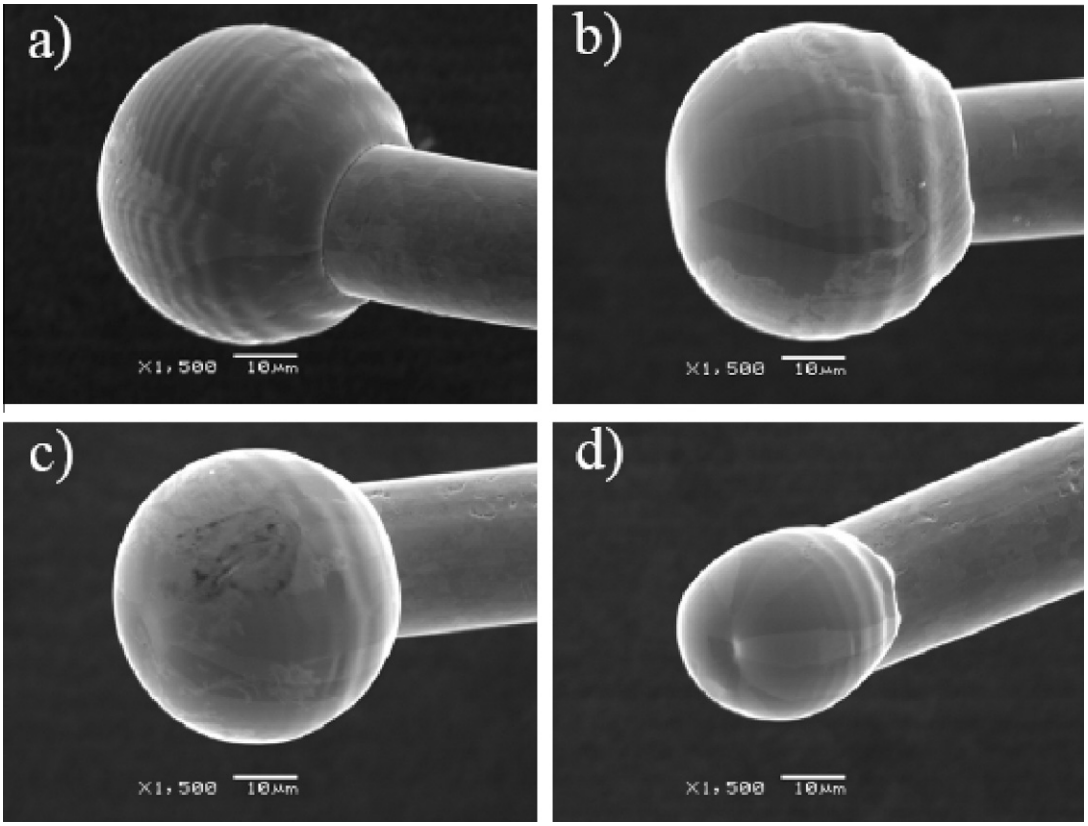

Fig. 10. SEM images of Au FABs produced in forming gas at flow rates of: (a) 0.25 l/min, (b) 0.4 l/min, (c) 0.6 l/min, and (d) 0.8 l/min.

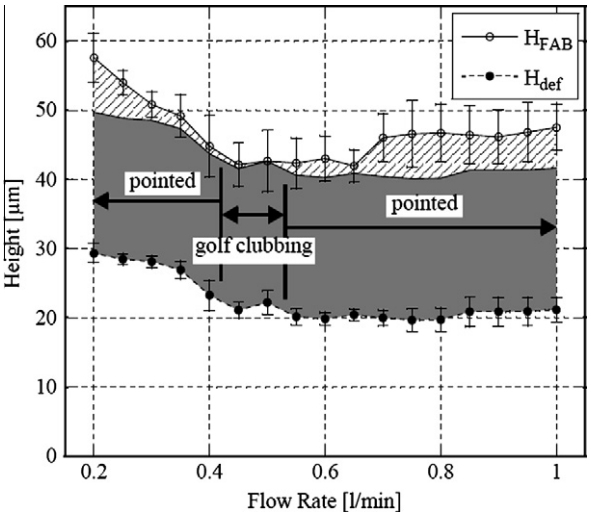

Fig. 11. Cu1 wire height measurements from online FAB characterization in N_2 gas. The mis-shaped FAB area is identified by the hatched region.

The SEM images of the Au FABs are shown in Fig. 16. Spherical FABs are produced up to 0.35 l/min as shown in Fig. 16a and b. At flow rates above 0.4 l/min the FABs begin to become golf-clubbed as shown in Fig. 16c. Above a flow rate of 0.4 l/min spherical FABs can no longer be formed as shown in Fig. 16d.

The H_{FAB} and H_{FAB}^{Trend} values are similar for flow rates up to 0.35 l/min as shown in Fig. 15. Above 0.35 l/min where golf-clubbed FABs are observed the mis-shaped FAB area increases and the slopes of both the H_{FAB} and H_{def} trends change abruptly.

3.3. Measured forced convective cooling

The thermocouple measurements taken from the EFO site at various flow rates for both forming gas and N_2 gas are shown in Fig. 17. With the heating block kept at 220 °C during bonding and room temperature is approximately 21 °C the EFO site is at a temperature of 59 °C when the gas flow rate is 0 l/min. As the flow rate is increased to 0.65 l/min the temperature at the EFO site decreases to temperatures of 40 °C and 42.5 °C in forming gas and N_2 gas, respectively. For flow rates above 0.65 l/min the temperatures increases abruptly to 45 °C in forming gas and 48 °C in N_2 gas. It is suspected that these increases are due to the gas flow changing from laminar to turbulent.

4. Discussion

4.1. Mechanisms for FAB defects

Heavy copper oxide identified by a scale-like texture on the FAB surface in Figs. 5 and 12 can cause the surface tension of the molten Cu ball to change. The pointed FAB shape as observed with the Cu1 wire is a result of a change in surface tension of the molten ball during the formation of the FAB. Metal oxides generally have a higher melting point and lower surface tension [13]. Therefore, during solidification the oxide on the molten Cu will form first, affecting the geometry of the FAB as the molten Cu rolls up due to surface tension [13].

Another possible mechanism for the formation of pointed FABs is forced convective cooling caused by the shielding gas flow [2,13]. The surface solidifies prematurely which again effects how the molten metal rolls up during solidification. The forced convective cooling effect of the shielding gas flow can decrease the bulk

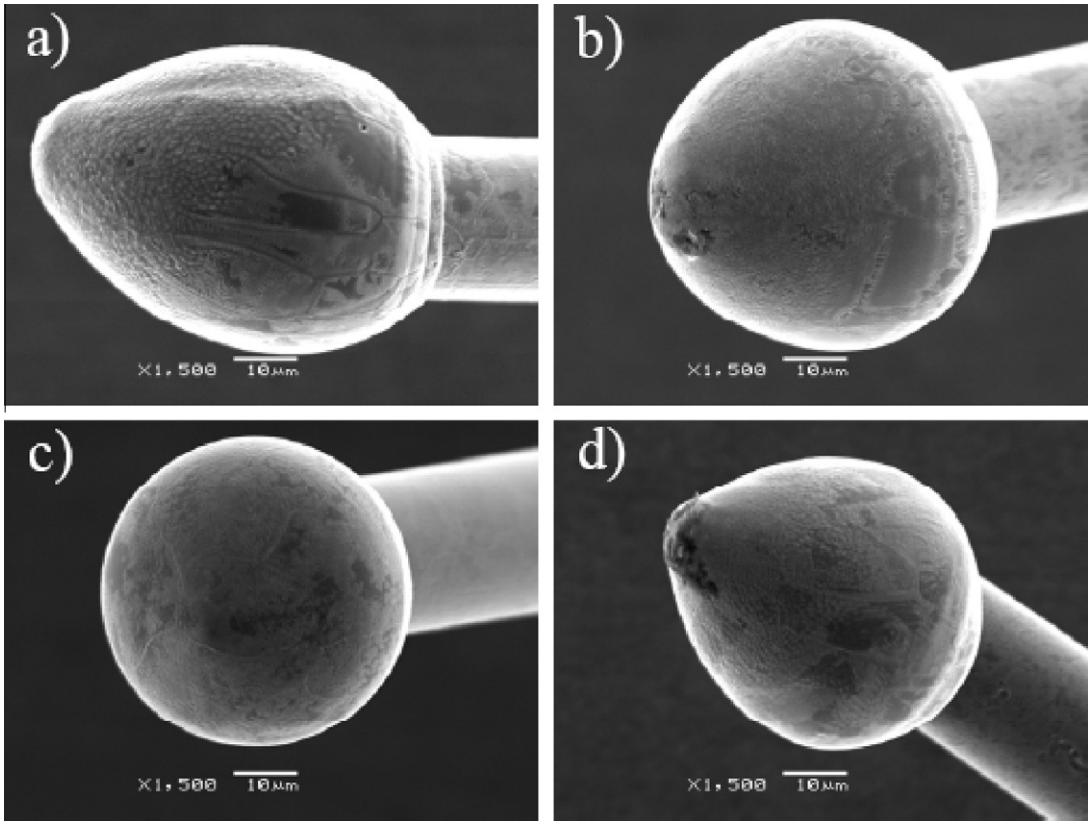

Fig. 12. SEM images of Cu1 FABs produced in N_2 gas at flow rates of: (a) 0.2 l/min, (b) 0.35 l/min, (c) 0.55 l/min, and (d) 0.7 l/min.

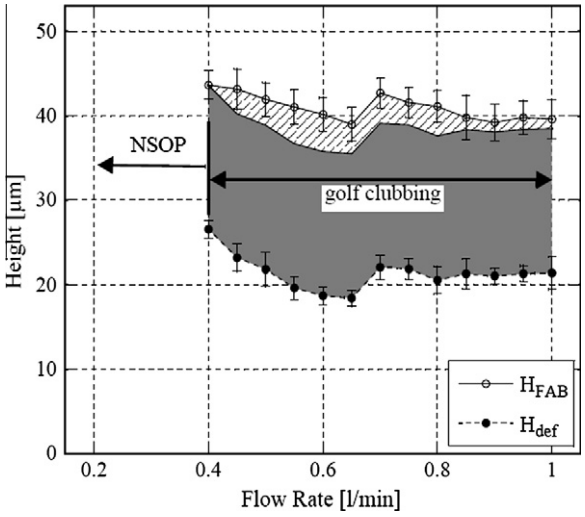

Fig. 13. Cu2 wire height measurements from online FAB characterization in N_2 gas. The mis-shaped FAB area is identified by the hatched region.

temperature of a thermocouple at the EFO site by up to 19 °C as shown in Fig. 17. The surface temperature decrease is expected to be substantially larger. An increase in temperature gradient between the molten metal and the environment increases the likelihood of premature solidification on the surface of the molten metal. Therefore, this convective cooling effect may have played a role in the pointed FABs seen at high flow rates of both forming gas and N_2 gas for the Cu1 wire.

Several different mechanisms have been proposed for the formation of golf-clubbed FABs. Hang [2] proposed that factors such as energy input during EFO, gap length between the electrode and the wire tail, high gas flow rates, as well as the condition of the wire tail can cause golf-clubbed FABs. Energy input during EFO and shielding gas flow rates were also suggested to be a cause of golf-clubbed FABs [9].

In this study only the effects of flow rate and gas type are directly linked to golf-clubbing since the EFO parameters have been kept constant. It is found that golf-clubbed FABs appear for both Cu2 and the Au wires at high flow rates of both forming gas and N_2 gas as shown in Figs. 8, 10, 14 and 16. At high flow rates both the drag force on the wire tail and molten metal ball could result in golf-clubbing. If the wire tail is pushed away from the electrode by the gas flow the gap will increase, which as observed in [2] leads to golf-club defects. Also, the drag force on the molten metal itself can cause the solidifying metal ball to freeze off-center on the wire. In contrast, with Cu1 pointed shapes instead of golf-clubbed shapes are observed under these conditions.

Since the EFO current and firing times are kept constant in this study, the atmosphere that the FAB is formed in is the other significant variable that affects the energy input during EFO. As the flow rate is increased the convective cooling effect increases causing the removal of energy from the EFO site and again a lower energy input leads to under-formed FABs that are golf-clubbed [2]. Also, with different flow rates the composition of the atmosphere at the EFO site will change which can have an effect on the energy transferred to the wire tail via the plasma during EFO.

At flow rates above 0.65 l/min for each of the Cu wire types studied, the EFO is observed to be unstable. The EFO site temperature abruptly rises as the gas flow rises above 0.65 l/min. Both of these observations can be explained by a change in flow type above the 0.65 l/min threshold. If the flow does in fact become more turbulent at this flow rate, the mixing effect between the air and the shielding gas as well as the convective cooling effect will increase.

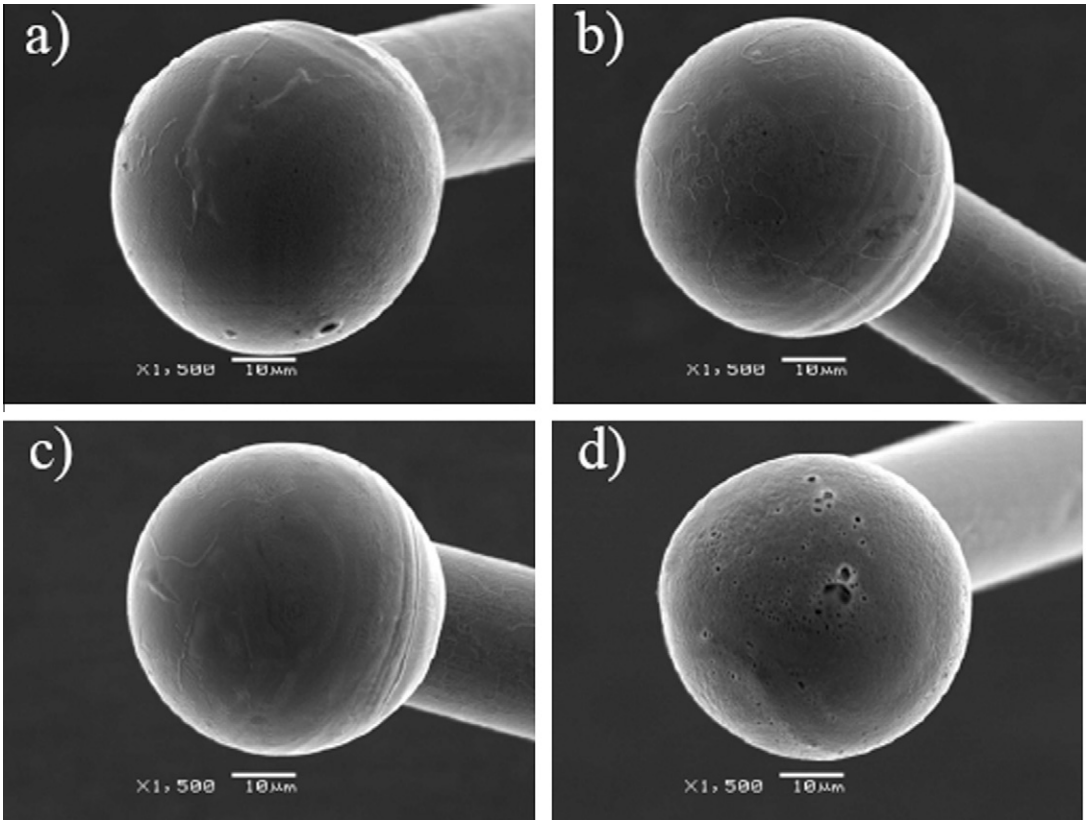

Fig. 14. SEM images of Cu2 FABs produced in N_2 gas at flow rates of: (a) 0.2 l/min, (b) 0.5 l/min, (c) 0.6 l/min, and (d) 0.75 l/min.

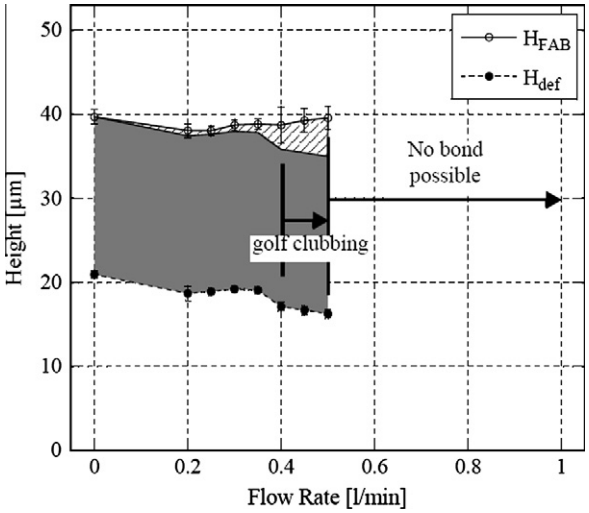

Fig. 15. Au wire height measurements from online FAB characterization in N_2 gas. The mis-shaped FAB area is identified by the hatched region.

With this increased mixing of the shielding gas with the air, the shielding provided by the gasses will lose its effect and oxidation will again occur. In Figs. 5, 8, 12 and 14 the increased oxidation can be easily identified at these high flow rates leading to instability in the EFO process and FAB defects.

4.2. FAB formation in forming gas compared to in nitrogen gas

The 5% H_2 in the forming gas helps reduce the Cu oxide during the EFO process and improves the Cu FAB quality [2,9,11,13]. The higher quality in Cu FABs is evident for both the Cu1 and Cu2 wires. For the Cu1 wire, less oxide is evident on the FAB surface when comparing the FABs formed in forming gas and N_2 gas as shown in Figs. 5 and 12, respectively. Also, the Cu2 wire has less surface oxide when the FABs are produced in forming gas rather than N_2 gas as shown in Figs. 8 and 14, respectively. Spherical FABs with insignificant surface oxide were only produced in forming gas for both Cu wires.

In addition to the reduction of Cu oxide, the H_2 added to the forming gas also provides additional thermal energy to the EFO process [9,13]. This added thermal energy is visualized in Figs. 4, 7 and 9 from flow rates of 0 l/min to approximately 0.3 l/min where the H_{FAB} measurements increase with increasing flow rate. The size of the FAB increases with the amount of H_2 present during EFO [13]. Above a flow rate of 0.3 l/min the convective cooling effect is hypothesized to take over and the FAB size again decreases [13]. The increase in H_{FAB} is not observed when the FABs are formed in N_2 gas as shown in Figs. 11, 13 and 15. These results are similar to those found in [13] and further indicate that the additional heat input is due to the addition of 5% H_2 to the forming gas.

The thermal energy provided by the forming gas containing H_2 gas could be a result of the reduction of the Cu oxide or by the rapid reaction/combustion of H_2 with stray oxygen [13]. The reduction reactions between hydrogen and Cu oxides are exothermic and therefore provide thermal energy. As found in [13], an increase in H_{FAB} was also observed for Au wire as shown in Fig. 9, where no reduction reactions occur. Therefore, the reduction of oxides is not likely the only source of additional thermal energy supplied by the H_2 gas. Since no oxidation or reduction reactions occur during the formation of the Au FAB, less thermal energy is available during EFO. As shown in Fig. 10 and Fig. 16, the Au FAB can no longer be formed at flow rates above 0.8 l/min and 0.5 l/min for FABs produced in forming gas and N_2 gas, respectively. The additional

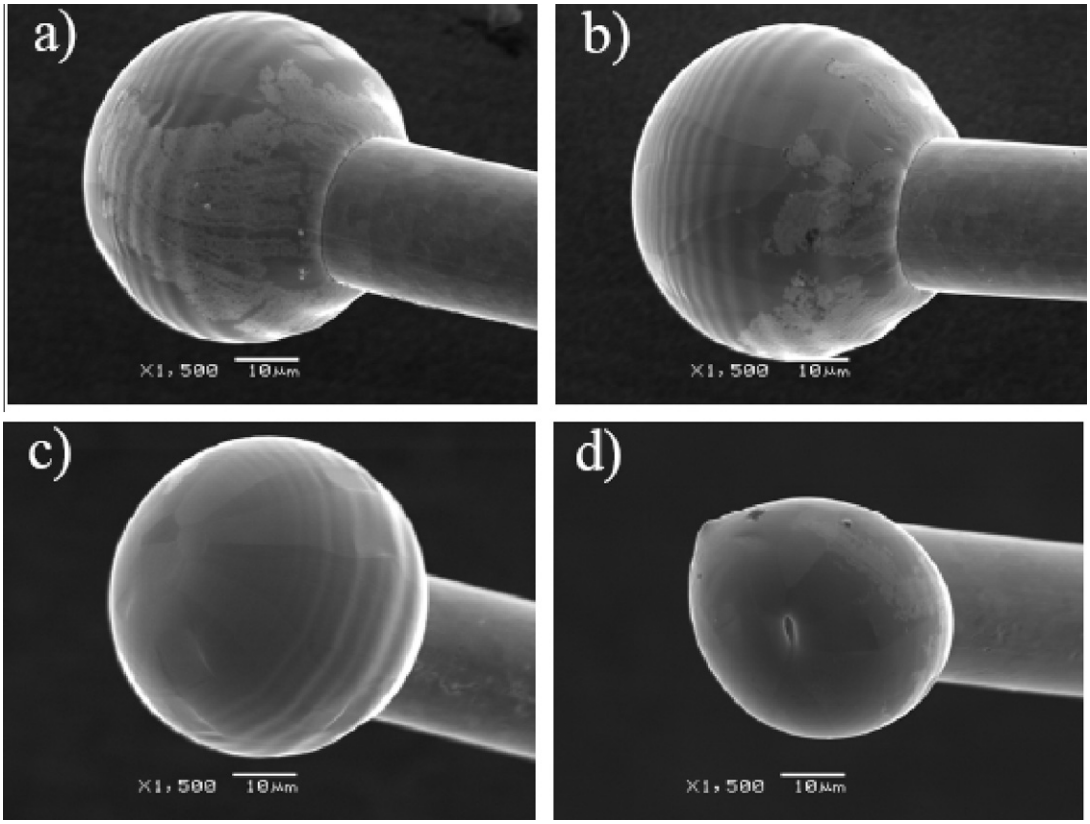

Fig. 16. SEM images of Au FABs produced in N_2 gas at flow rates of: (a) 0.2 l/min, (b) 0.35 l/min, (c) 0.45 l/min, and (d) 0.6 l/min.

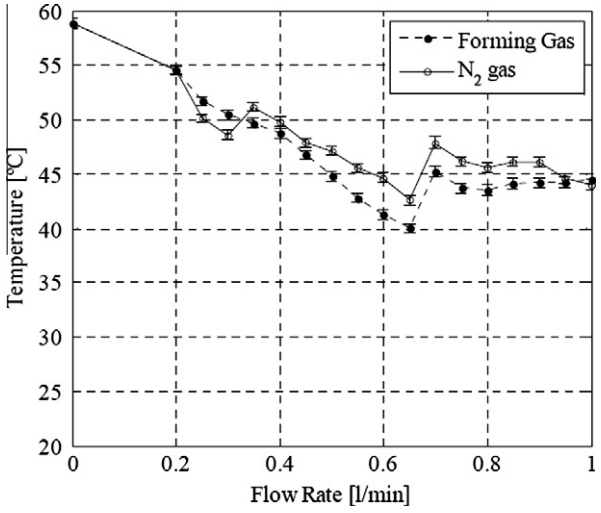

Fig. 17. Temperature at EFO site with increasing flow rates of N_2 gas and forming gas.

thermal energy due to the rapid reaction/combustion of H_2 with stray oxygen is a possible explanation for the ability to form Au FABs up to flow rates of 0.8 l/min in forming gas while FABs can only be formed with flow rates up to 0.5 l/min in N_2 gas. Another possible explanation is a change in the ionization potential of the gas due to the change in gas chemistry.

4.3. Characterizing FABs with the online method

The purpose of the online characterization method is to eliminate the need for manual analysis methods such as SEM analysis. Online characterization can be less time consuming than taking SEM images of every FAB produced during process optimization of the EFO process. The trends in H_{FAB} and H_{def} are used to characterize the FAB of a wire. Sudden changes in the slope of the H_{FAB} and H_{def} trends, large differences in H_{FAB} and the H_{FAB}^{Trend} values, and a large standard deviation of the H_{FAB} measurements are all indications of unstable EFO processes where FAB defects occur. Also, the size of the mis-shaped FAB area can be used as an approximation of the robustness of a wire material during EFO.

For FABs produced in forming gas, abrupt changes of the H_{FAB} measurements with increasing flow rate and large differences in H_{FAB} and H_{FAB}^{Trend} illustrated by large mis-shaped FAB areas, indicate pointed FABs. Golf-clubbed defects can be identified by the change in slope to approximately zero as seen for both the Cu2 and Au wire results shown in Figs. 7 and 9. The mis-shaped FAB area cannot always be used to identify FAB defects as shown for the Cu2 wire where golf-clubbed defects occur above flow rates of 0.65 l/min and the H_{FAB} measurements and the H_{FAB}^{Trend} values remain similar.

The Cu FABs produced in N_2 gas are found to be defective and in most cases have excessive oxidation on their surface. For both the Cu1 and Cu2 wires the FAB defects are identified by abrupt changes in H_{FAB}, large mis-shaped FAB area, and the large standard deviation of the measured H_{FAB} values at each flow rates. If the FABs are defective at all flow rates, the H_{FAB}^{Trend} value cannot be used to identify the flow rates where spherical FABs result.

The online characterization results for Au FABs formed in both forming gas and N_2 gas are similar. Golf-clubbed defects are identified by the slope of the H_{FAB} measurements decreasing to approximately zero and a large increase in mis-shape FAB area at higher flow rates. The effects of H_2 on the Au FAB size is identified when comparing the online characterization results of Au FABs formed in forming gas to those formed in N_2 gas.

It is important to note that the calculated H_{FAB}^{Trend} value and therefore, mis-shaped FAB area, are approximations and should only be used as indications that defective FABs are being produced. Changes in the FAB volume, hardness, or deformability with changing flow rate can affect the measured H_{def} value. The difference between H_{FAB} and H_{def} is not necessarily a constant.

5. Conclusions

The effectiveness of the online FAB characterization is demonstrated and the FAB formation during the EFO process has been studied using both forming gas and N_2 gas. The online method identifies the gas flow rates required to produce acceptable Cu FABs and is therefore a useful tool for optimizing the shielding gas flow rate. The flow rate should be optimized for each new wire type used.

The addition of H_2 to the gas mixture provides additional thermal energy to the EFO process and reduces the Cu oxide during EFO decreasing the likelihood of forming defective Cu FABs. The additional thermal energy is determined to not be only a product of the reduction of oxides but of at least one other reason.

Acknowledgements

This work is supported by the Natural Science and Engineering Research Council (NSERC) of Canada, Initiative for Automotive Innovation (IAMI), Ontario Centers of Excellence (OCE), Microbonds Inc., Markham, Canada, and MK Electron Co. Ltd., Yongin, Korea.

References

[1] Zhou Y. Microjoining and nanojoining. Cambridge (England): Woodhead Publishing Ltd.; 2008.
[2] Hang C, Wang C, Shi M, Wu X, Wang H. Study of copper free air ball in thermosonic copper ball bonding. In: Proceedings of IEEE 6th international conference on electronics packaging technology; 2005. p. 414–8.
[3] Harman G. Wire bonding in microelectronics materials, processes, reliability, and yield. 2nd ed. New York: McGraw-Hill; 1997.
[4] Shah A, Mayer M, Zhou Y, Hong SJ, Moon JT. Reduction of underpad stress in thermosonic copper ball bonding. In: Proceedings of the 58th IEEE electronic components and technology conference; 2008. p. 2123–30.
[5] Zhong ZW, Ho HM, Tan YC, Tan WC, Goh HM, Toh BH, et al. Microelectron Eng 2007;84:368–74.
[6] Onuki J, Koizumi M, Suzuki H. J Appl Phys 1990;68(11):5610–4.
[7] Pequegnat A, Hang CJ, Mayer M, Zhou Y, Moon JT, Persic J. J Mater Sci: Mater Electron 2008:1144–9.
[8] Caers JF, Bischoff A, Falk J, Roggen J. Conditions for reliable ball-wedge copper wire bonding. In: Proceedings of IEEE Japan international electronics manufacturing technology symposium; 1993. p. 312–5.
[9] Xu H, Liu C, Silberschmidt V, Wang H. Effects of process parameters on bondability in thermosonic copper ball bonding. In: Proceedings of electronic components and technology conference; 2008. p. 1424–30.
[10] Toyozawa K, Fujita K, Minamide S, Maeda T. IEEE Trans Compon Hybrids Manuf Technol 1990;13(4):667–72.
[11] Khoury S, Burkhard D, Galloway D, Scharr T. IEEE Trans Compon Hybrids Manuf Technol 1990;13(4):673–81.
[12] Sripada S, Cohen I, Ayyaswamy P. J Heat Transfer 2003;125:661–8.
[13] Ho HM, Tan J, Tan YC, Toh BH, Xavier P. Modeling energy transfer to copper wire for bonding in an inert environment. In: Proceedings of IEEE electronics packaging technology conference; 2005. p. 292–7.
[14] Hang CJ, Lum I, Lee J, Mayer M, Wang CQ, Zhou Y, et al. Microelectron Eng 2008;85:1795–803.
[15] Lee J, Mayer M, Zhou Y, Hong SJ. Microelectron J 2007;38:842–7.
[16] Pequegnat A, Mayer M, Persic J, Zhou Y. Accelerated characterization of bonding wire materials. In: The proceedings of IMAPS 42nd international symposium on microelectronics; 2009. p. 367–73.
[17] Lum I, Hang CJ, Mayer M, Zhou Y. J Electron Mater 2009;38(5):647–54.